EUROPEAN ORGANIZATION FOR NUCLEAR RESEARCH

Proposal to the ISOLDE and Neutron Time-of-Flight Committee

Probing the doubly magic shell closure at ^{132}Sn by Coulomb excitation of neutron-rich ^{130,134}Sn isotopes

12 May 2021

P. Reiter[1], Th. Kröll[2], M. Droste[1], K. Arnswald[1], A. Blazhev[1], H. Hess[1], H. Kleis[1], N. Warr[1], C. Henrich[2], A.-L. Hartig[2], H.-B. Rhee[2], M. Rudigier[2], C. Sürder[2], I. Homm[2], N. Pietralla[2], M. Scheck[3], R. Gernhäuser[4], H. De Witte[5], M. Huyse[5], P. Van Duppen[5], P. Thirolf[6], L. P. Gaffney[7], A. Jungclaus[8], K. Wimmer[8,9], G. Georgiev[10], J. Cederkäll[11], G. Rainovski[12], D. Kocheva[12], K. Gladnishki[12], D. Bucurescu[13], N. Mărginean[13], R. Mărginean[13], D. Deleanu[13], A. Negret[13], D. Balabanski[14], K. Hadynska-Klek[15], K. Wrzosek-Lipska[15], P. J. Napiorkowski[15], M. Komorowska[15], D. Mücher[16], V. Bildstein[16], R. Chapman[3], T. Grahn[17,18], P. T. Greenlees[17,18], A. Illana[17,18], J. Pakarinen[17,18], P. Rahkila[17,18], R. Lozeva[19], A. Andreyev[20], L. M. Fraile[21], J. M. Allmond[22], A. Stuchbery[23], and the MINIBALL and HIE-ISOLDE collaborations

[1] *Univ. of Cologne, Germany*; [2] *TU Darmstadt, Germany*; [3] *Univ. West of Scotland, Paisley, UK*; [4] *TU München, Germany*; [5] *KU Leuven, Belgium*; [6] *LMU München, Germany*; [7] *Univ. of Liverpool, UK*; [8] *IEM CSIC, Madrid, Spain*; [9] *Univ. of Tokyo, Japan*; [10] *IJCLab, Orsay, France*; [11] *Univ. of Lund, Sweden*; [12] *Univ. of Sofia, Bulgaria*; [13] *IFIN-HH, Bucharest, Romania*; [14] *ELI-NP, Măgurele, Romania*; [15] *Heavy Ion Laboratory, Univ. of Warsaw,Poland*; [16] *Univ. of Guelph, Canada*; [17] *Univ. of Jyväskylä, Finland*; [18] *Helsinki Institute of Physics, Finland*; [19] *IJCLab, Universit Paris-Saclay, Orsay, France*; [20] *Univ. of York, UK*; [21] *UC Madrid, Spain*; [22] *Oak Ridge National Laboratory, USA*; [23] Australian National University, Canberra, Australia;

Spokespersons: P. Reiter [preiter@ikp.uni-koeln.de], Th. Kröll [tkroell@ikp.tu-darmstadt.de]
Contact person: B. Olaizola [Bruno.Olaizola@cern.ch]

CERN-INTC-2021-039 / INTC-P-608
12/05/2021

Abstract: We propose to study excited states in the isotopes ^{130,134}Sn by γ-ray spectroscopy following "safe" Coulomb excitation. The experiment aims to investigate the evolution of collectivity and nuclear structure around and the magic-shell closure at $N = 82$ for tin isotopes ($Z = 50$) via the determination of the reduced transition strength, in particular $B(E2; 0^+_{\text{g.s.}} \rightarrow 2^+_1)$ and for the first time in this mass region $B(E2; 2^+_1 \rightarrow 4^+_1)$ values. In addition, the experiment aims to investigate the evolution of quadrupole collectivity in the vicinity of the magic shell closure at $N = 82$ by the determination of electric quadrupole moments Q_2 and, potentially, $B(E3)$ values. Most advanced shell-model calculations using realistic interactions predict enhanced collectivity in the neighbouring isotopes of ^{132}Sn. These predictions await experimental verification. Moreover, a puzzling discrepancy between previous measurements in the two key nuclei ^{130,134}Sn and latest theoretical results needs to be resolved by precise and accurate new experiments.

Requested shifts: [15+15] shifts
Installation: [MINIBALL + CD (C-REX)]

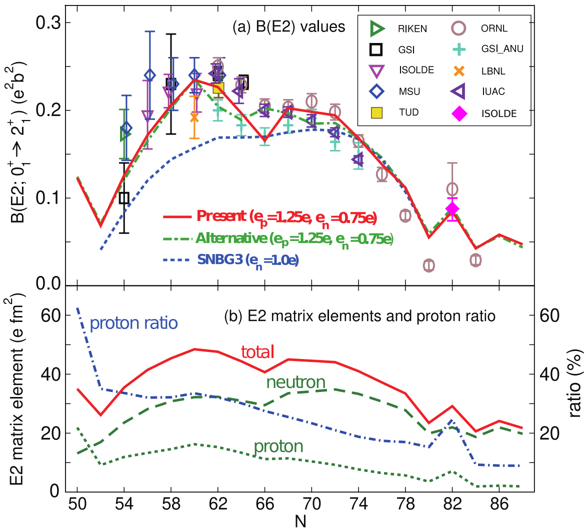

Figure 1: The $B(E2, 0^+_{\text{g.s.}} \to 2^+_1)$ systematics for the Sn isotopes. (a) calculated and measured $B(E2)$ values, and (b) $E2$ matrix elements and proton ratio (%). Experimental data are indicated by symbols shown in the inset. Figure taken from Ref. [2].

1 Motivation and Physics Case

The two doubly magic nuclei ^{100}Sn and ^{132}Sn are subject of great and persisting experimental as well as theoretical interest. Moreover, the region around ^{132}Sn is the focus of many efforts since the astrophysical r process is expected to pass through this region. The understanding of the nuclear structure has an impact on the description of the $A \approx 130$ peak in the solar element abundances[1].

Advanced techniques and new facilities using radioactive ion beams, allow to obtain new data which offer the opportunity to test recent theoretical models. Latest state-of-the-art Monte-Carlo Shell-Model (MCSM) calculations are performed with an unprecedented large configuration space with eight single-particle orbits for protons and neutrons [2]. This calculation allowed a detailed description of the shape evolution along the tin isotopic chain between $^{100-138}$Sn with one fixed Hamiltonian. Remarkably, nearly all the calculated $B(E2, 0^+_{\text{g.s.}} \to 2^+_1)$ values follow closely the experimental values within their experimental uncertainties. In this way, the long term problem of the enhanced quadrupole collectivity on the neutron-deficient side (see for example [3, 4, 5]) and the non-parabolic behaviour of these $B(E2)$ values was resolved.

As the $Z = 50$ gap is large and almost constant and large over a wide mass range, proton excitations across it require large excitation energy. The first excited 2^+_1 levels of Sn have excitation energies of ~ 1.2 MeV and vary only smoothly along the whole Sn chain between the two doubly-magic Sn nuclei. These 2^+ levels are likely almost of pure neutron character. The small rise and fall of the state around $N = 64$ is caused by the presence of a weak sub-shell closure. The constancy of the 2^+_1 energies at each side of the sub-shell closure confirms that pairing correlations dilute shell occupancies and generate 2^+_1 states of similar configurations. The increase of the 2^+_1 state for the ^{132}Sn nucleus arises from the fact that both neutron and proton excitations across the $Z = 50$ and $N = 82$ shell gaps require high energies. Therefore, the ^{132}Sn nucleus exhibits the characteristics of a doubly-magic nucleus with a high energy for the first excited states. The first 2^+_1 state is no longer of pure neutron origin, but contains proton excitations as well. These proton excitations cause an enhanced transition probability with respect to the neighbouring even-even isotopes. Experimental $B(E2)$ values are shown in Fig. 1 (taken from Ref. [2]) for the Sn isotopes. The data points for unstable nuclei are obtained from Coulomb excitation using radioactive ion beams.

For $N > 66$, the $B(E2)$ value follows the parabolic trend of the generalized seniority scheme with the exception of ^{132}Sn. The wave function of the 2^+_1 states of tin isotopes is dominated by neutron excitations. However, at ^{132}Sn, both proton and neutron low-energy excitations are hin-

[1] In 2017, for the first time observations confirmed a binary neutron star merger as an astrophysical site of the r-process with the light curves as indicator for the composition of isotopes produced and their decay [1].

dered due to the presence of shell gaps. Therefore, the energy of the 2_1^+ state suddenly increases and its wave function has mixed components, both from neutron and proton, causing the local increase of the $B(E2)$ value. Beyond the $N = 82$ shell closure, the neutron excitations dominate again. Very small $B(E2)$ values were measured in ^{130}Sn and ^{134}Sn nuclei and preliminary results were published in conference proceedings [6, 7].

For doubly magic ^{132}Sn, a recent experiment performed at HIE-ISOLDE with the MINIBALL & C-REX set-up has revealed enhanced $E2$ and $E3$ strengths. The measured $B(E2)$ value of 0.087 e^2b^2 [8] compares well with the theoretical value of 0.085 e^2b^2 [2]. However, at $N = 80$ and $N = 84$ the neighbours of ^{132}Sn, a clear discrepancy occurs between the MCSM calculations and the experimental $B(E2)$ values. The experimental values for ^{130,134}Sn are taken from preliminary results published in conference proceeding (see Fig. 1). It is noteworthy that the excitation energy of the first 2^+ state in ^{130}Sn is 1221 keV while in ^{134}Sn it is only 725.6 keV. In contrast, the measured $B(E2; 0^+_{\mathrm{gs}} \rightarrow 2^+)$ value of 0.029(5) e^2b^2 for ^{134}Sn is very similar to the value for the two-hole nucleus ^{130}Sn [7]. The results of the Tokyo shell-model group yield larger $B(E2, 0^+_{\mathrm{g.s.}} \rightarrow 2^+_1)$ values of 0.055, 0.044 and 0.056 e^2b^2 for ^{130}Sn, ^{134}Sn and ^{136}Sn, respectively.

Recent large-scale shell-model calculation including the large model space spanned by $0h_{11/2}$, $1f_{7/2}$, $0h_{9/2}$, $1f_{5/2}$, $2p_{3/2}$, $2p_{1/2}$ orbitals for neutrons, and $0g_{9/2}$, $0g_{7/2}$, $1d_{5/2}$, $1d_{3/2}$, $2s_{1/2}$ orbitals for protons above the inert core of ^{110}Zr, were performed by N. Houda and F. Nowacki from the Université de Strasbourg. The $B(E2, 0^+_{\mathrm{g.s.}} \rightarrow 2^+_1)$ strengths from this large-scale shell-model calculation yield 0.028 and 0.027 e^2b^2 for ^{130}Sn and ^{134}Sn, respectively. This is in agreement with the preliminary experimental values yielding 0.023(5) and 0.029(5) e^2b^2.

Predictions for neutron-rich Sn nuclei were also made employing a separable quadrupole-plus-pairing Hamiltonian and the Quasi-Particle Random-phase Approximation (QRPA) [9]. Excitation energies, $B(E2, 0^+_{\mathrm{g.s.}} \rightarrow 2^+_1)$ strengths, and g factors for the first 2_1^+ states near ^{132}Sn ($Z > 50$) were calculated. A local maximum of the $B(E2, 0^+_{\mathrm{g.s.}} \rightarrow 2^+_1)$ value at $N = 82$ and a symmetric behaviour with respect to the $N = 80$ and $N = 84$ neighbours is predicted. For the ^{130,132,134}Sn isotopes the theoretical $B(E2)$ values are also considerable lower than the preliminary determined experimental values.

Another important aspect of the following proposal is related to the long-standing problem of how accurate the description of nuclear structure properties is provided by realistic shell-model interactions employing two-body matrix elements deduced from a realistic nucleon-nucleon interaction. This is considered a more fundamental approach to the nuclear shell model than the calculations which are based on empirical effective interactions containing several adjustable parameters.

Various approaches have been used to generate shell-model interactions capable to predict properties of neutron-rich nuclei beyond $N = 82$ using either empirical approaches (e.g. SMPN) [10] or realistic free nucleon-nucleon potentials (e.g. CD-Bonn), renormalized by either G-matrix (e.g. CWG) [11] or $V_{low\ k}$ methods [12]. For Sn isotopes, the calculations with empirical interactions predicts even a new shell closure at $N = 90$ as the $\nu f_{7/2}$ orbital is filled, whereas the calculations with realistic interactions do not find such an effect. The $\nu f_{7/2}$ orbit being filled beyond $N = 82$ shows an interesting analogy with the Ca isotopic chain where a $\nu f_{7/2}$ orbital is filled between $N = 20$ and $N = 28$. There was the long-standing problem that realistic interactions were not able to reproduce the shell closure at $N = 28$. This has been resolved by including three-body forces [13]. Indeed, a shell closure at $N = 90$ in ^{140}Sn is predicted including three-body forces by calculations based on realistic interactions (CWG3M) [14].

To judge the predictive power of new calculations at this critical position in the chart of nuclei, new measurements with high accuracy are needed. Therefore, we propose to study excited states in the isotopes ^{130,134}Sn by γ-ray spectroscopy following 'safe' Coulomb excitation in order to obtain firm values and to resolve the puzzling discrepancy for these crucial isotopes.

Beyond the specific measurements of $B(E2, 0^+ \rightarrow 2^+)$, knowledge of the structure of the Sn isotopes is particularly important to test the neutron-neutron part of shell-model interactions as proton-proton and proton-neutron terms do not contribute at low energies and, therefore,

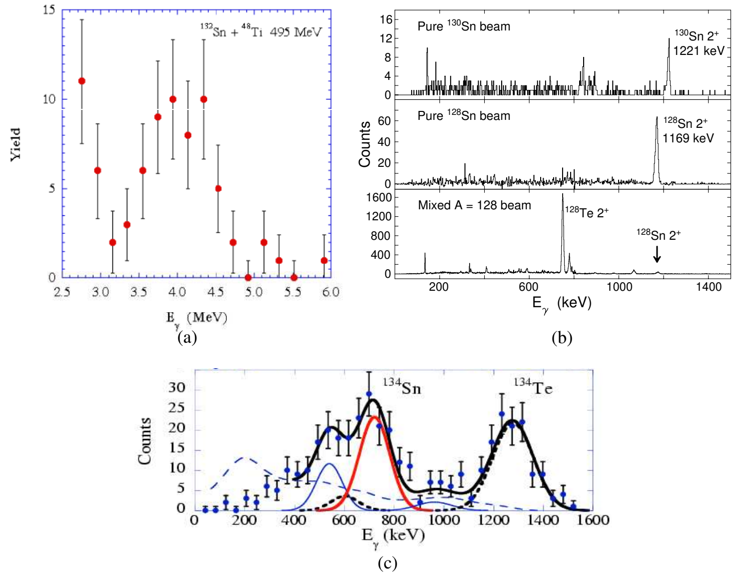

Figure 2: (a) Yield of photons around 4 MeV in ^{132}Sn Coulomb excitation. Figure taken from Ref. [7]. (b) γ-ray after Coulomb excitation of ^{128,130}Sn recorded with the CLARION array. $2^+_1 \rightarrow 0^+_{\mathrm{g.s.}}$ transitions are labeled. Figure taken from Ref. [6]. (c) γ-ray spectrum recorded with the BaF_2 array TAMU after Coulomb excitation of ^{134}Sn. Contaminations stemming from ^{134}Ba and ^{134}Te are clearly visible. Figure adapted from Ref. [7].

low-lying states have a pure neutron character. The results of the proposed experiment will aid the understanding of the evolution of neutron-neutron two-body matrix elements in nuclei with large neutron excess.

1.1 Status of previous experiments

At the Holifield Radioactive Ion Beam Facility at ORNL first measurements of the $B(E2, 0^+_{\mathrm{g.s.}} \rightarrow 2^+_1)$ values for a number of nuclei in the vicinity of the $N = 82$ shell closure were performed. Two experiments were optimized to determine the transition probability of the first excited 2^+_1 state in ^{128,130,132}Sn and ^{134}Sn [6, 7, 15]. The $B(E2, 0^+_{\mathrm{g.s.}} \rightarrow 2^+_1)$ values in ^{128}Sn and ^{130}Sn were measured employing the CLARION HPGe detector array in conjunction with the HyBall particle identification.

The large excitation energy (4041 keV) of the 2^+_1 state in ^{132}Sn and small excitation cross-section, together with the available beam intensity made the experiment very challenging. To cope with the low γ-ray count rate an efficient BaF_2 array was employed for this measurement and not the CLARION Ge spectrometer. The same BaF_2 array was used to measure the γ rays after the Coulomb excitation of ^{134}Sn. The results of the Coulomb excitation experiment were reported in three different conference proceedings contributions [6, 7, 15] but not in peer reviewed journals.

The most detailed report on the ^{132,134}Sn experiment is given in Ref. [7], here a spectrum from the BaF_2 spectrometer is shown in Fig 1.1 (a) and (c). The authors made aware that: 'This preliminary analysis does not yet include a complete experimental calibration of the photon detector efficiency.' [7]. From this work the result for the $B(E2, 0^+_{\mathrm{g.s.}} \rightarrow 2^+_1)$ value of ^{132}Sn is given to be 0.11(3) e^2b^2, whereas the value for ^{134}Sn is 0.029(5) e^2b^2. In addition, the beam purity of ^{134}Sn amounted to 25% with a contamination of around 62% of ^{134}Te, 12% ^{134}Sb and 0.5% ^{134}Ba, which complicated the analysis (see Fig. 1.1 (a) and (c)). For the ^{130}Sn measurement only a preliminary value of 0.023(5) e^2b^2 and one spectrum is shown in Ref. [6] (c.f. Fig. 1.1 (b)).

2 'Safe' Coulomb excitation of ^{130,134}Sn

Coulomb excitation of the first excited 2^+ and 4^+ state in ^{130,134}Sn is proposed. High beam intensities and purities for radioactive tin ions are based on molecular SnS beams. Beam intensities of ^{130,132}Sn of more than $3.0 \cdot 10^{+7}$ ions/C were extracted from ISOLDE targets. Beam energies of 4.4 MeV/u will be provided by the HIE-ISOLDE accelerator. This will allow the usage of a high Z target, like ^{206}Pb, target for Coulomb excitation. Large cross sections can be exploited for pure electromagnetic excitation at a distance of closest approach well above the criterion for safe Coulex. The γ-rays from ^{130,134}Sn will be recorded with the MINIBALL spectrometer [16] and a coincident scattered particle detected by a position sensitive double sided silicon detectors in forward direction or, optionally, C-REX a version of T-REX [17] with a large angular coverage. The scattered ^{130,134}Sn ions are kinematically separated from the recoiling target nuclei under forward angles by the CD (C-REX) silicon detectors.

The excitation cross section for Coulomb excitation depends not only on the transitional but also on the diagonal matrix elements, an effect known as reorientation. As the single- and multi-step processes and the reorientation effect depend on the scattering angle, a large coverage of scattering angles in the CM system is favourable. In the analysis, the data set is split in different angular bins. The matrix elements are then determined by a maximum likelihood fit.

The analysis of the excitation cross section will be performed relative to the excitation of the target. The cross section is maximised by using a high-Z ^{206}Pb target. The only state which will be excited ($E(2^+) = 803$ keV) is well separated from the expected γ-rays of ^{130,134}Sn, which are the $2^+ \to 0^+$ transitions at 1221.2 keV and 725.6 keV and the $4^+ \to 2^+$ transitions at 774.4 keV and 347.8 keV. The 3^- state in ^{206}Pb is above 2.6 MeV and decays by high-energy γ rays.

The "safe" energy for ^{130,134}Sn on lead is about 4.4 MeV/u ($\vartheta_{\mathrm{CM}} = 180°$). In Fig. 3, the calculated energies of the scattered projectiles and the recoiling target nuclei are shown. The energy loss in the target was calculated with SRIM2008 [18] and the pulse height deficit was included (Ref. [19]). It can be seen that the projectiles and the recoils are well separated below $\vartheta < 70°$. The use of a target thicker than 1 mg/cm^2 reduces the separation. But also 3 mg/cm^2 target of ^{206}Pb, that was employed in our previous experiment IS551 with a ^{132}Sn beam, did allow separation between scattered beam and target particles.

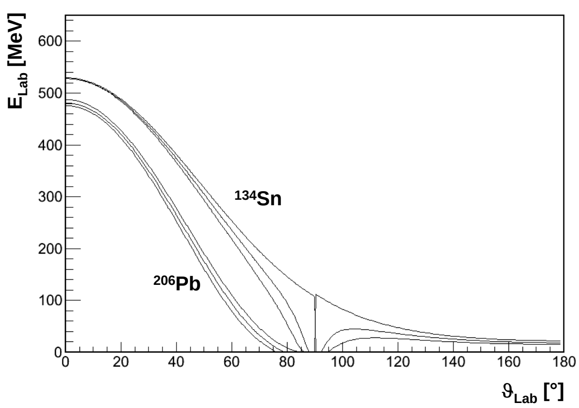

Figure 3: *Kinetic energies of scattered ^{134}Sn projectiles and recoiling ^{206}Pb target nuclei for an incident energy of 4.4 MeV/u and a target thickness of 1 mg/cm^2. The lines show the limiting cases of a scattering at the front, the middle, or the back layers of the target, respectively.*

Table 1 summarises the calculated cross sections for elastic scattering and the excitation of the first two states in ^{130,134}Sn. For ^{130}Sn we have taken the measured small $B(E2, 0^+_{\mathrm{g.s.}} \to 2^+_1)$ value from the ORNL experiment [7]. This value may be considered as a lower bound, theoretical predictions e.g. by [2] (see Fig. 1) are clearly enhanced. The matrix elements for ^{134}Sn are taken from Ref. [11]. Also this value lies well below the recent shell model prediction [2]. The different sensitivities on single- or multi-step excitation at different CM scattering angle regions, e.g. the ratio $\sigma(4^+)/\sigma(2^+)$, are obvious. The impact of the reorientation effect is estimated for ^{134}Sn assuming diagonal matrix elements of 0 eb and ± 0.5 eb for all states which results in cross section changes by up to 20 %, in particular at backward angles. The diagonal matrix elements may be expected to be small, e.g. in ^{124,126,128}Sn values compatible with zero have been found [20]. However, for ^{134}Sn a quite large $Q_2(2^+_1) = 1.6$ eb is predicted [12]. The cross section for the ^{206}Pb target excitation is on the order of 0.5 b.

As it can be seen from Table 1, we expect that for ^{130,134}Sn, the 2^+_1 and 4^+_1 states will be excited. Hence, the future analysis described above has to consider only two transitional and, at maximum, two diagonal matrix elements. In ^{134}Sn, the isomeric 6^+ state has no impact. Finally,

	$15^\circ < \vartheta_{\mathrm{Lab},3} < 50^\circ$ ($25^\circ < \vartheta_{\mathrm{CM}} < 80^\circ$)	$105^\circ < \vartheta_{\mathrm{Lab},4} < 172^\circ$ ($80^\circ < \vartheta_{\mathrm{CM}} < 150^\circ$)
Ruth	43	3
^{130}Sn: 2^+	0.13	0.09
4^+	0.00019	0.00046
^{134}Sn: 2^+	0.40(3)	0.32(8)
4^+	0.0026(2)	0.010(2)

Table 1: *Calculated cross sections, in [b], for a ^{130}Sn (^{134}Sn) beam at 556 MeV(573 MeV) on a lead target. The variation due to the reorientation effect is given in parenthesis (see text).*

in contrast to multiple Coulomb excitation of more collective nuclei no additional constraints from other experiments, like lifetimes, are required in order to simplify the analysis.

The beam composition will be determined from the characteristic γ-rays from the decay of the Sn, Sb and Te isotopes. For this purpose several techniques were established in previous MINIBALL experiments [8, 23, 24]. From our experience with A-Sn beams produced as ^{A}Sn^{34}S^{+1} molecular ions, we expect as contaminants the respective A-isobars, mainly ^{A}Sb, and isotopes with $A+34$, in particular $^{A+34}$Yb [8, 24]. The isotope ^{134}Sn ($T_{1/2} = 1.05$ s [25]) will decay to a small amount, about 10 %, similar to ^{142}Xe (1.23 s) measured 2016 [23], inside the EBIS adding to the contamination.

The ground state of isotope ^{130}Sn ($T_{1/2} = 3.72$ m [25]) will β decay into two excited 1^- states of ^{130}Sb. The consecutive γ decay is feeding solely into an isomeric 5^- state that decays ($T_{1/2} = 6.3$ m [25]) into ^{130}Sb and consecutively into the stable ^{130}Te. For the ^{130}Sn beam, also a considerable fraction of up to 50% is expected to be produced as a β decaying 7^- isomer (excitation energy 1946.88 keV, $T_{1/2} = 1.7$ m [25]). The beam fraction of this isomer will be determined by β decay properties. In contrast to the ground state decay of ^{130}Sn, the decay of the 7^- isomer populates excited states in ^{130}Sb which are completely different and which can be clearly identified by their distinct γ-ray decay sequence. These γ decays populate the ground state of ^{130}Sb ($T_{1/2} = 39.5$ m [25]) and not the isomeric 5^- state. A certain fraction of the 7^- isomer in ^{130}Sn decays directly into the 8^- ground state of ^{130}Sb and cannot be diagnosed via γ decay. To identify this fraction of the ^{130}Sn beam the consecutive β decays from the 8^- ground state and the isomeric 5^- state with its distinct adjacent γ-ray decay sequence in stable ^{130}Te will be exploited.

3 Rate estimate and beam time request

The Sn isotopes of interest are produced using a standard UC$_x$/graphite target irradiated with the proton beam from the PS Booster. In order to eliminate the Cs contamination, we will extract SnS$^+$ molecules which will be cracked afterwards in the EBIS. We will use isotopically enriched ^{34}S and produce a very clean $A = 168$ beam containing only ^{134}Sn^{34}S$^+$ molecules [26].

The isotopes ^{130,134}Sn decay to their respective Te isobars. The decay products involved with longest half-lifes are ^{134}I ($T_{1/2} = 52$ min), ^{134}Te ($T_{1/2} = 41.8$ min) and ^{130}Sb ($T_{1/2} = 39.5$ min). Therefore, activation by long-lived decay products is no issue for the experiment and radiation protection.

Latest ISOLDE yield measurements for Sn isotopes obtained reduced ion beam intensities compared to past experiments (see e.g. [27, 28]). A measured beam current of $3 \cdot 10^5$ ions/s was measured in 2016 for ^{132}Sn at the MINIBALL target [8]. This current value was a factor of 2-3 below the value extracted from the ISOLDE yield tables. Therefore, we employ a reduced beam current (factor of 2.5 lower) with respect to the ISOLDE yield tables for the rate estimate. Assuming a proton current of 2 μA and, conservatively, an efficiency of HIE-ISOLDE of 5% the following **beam currents are expected at the MINIBALL spectrometer: 10^6 ions/s for ^{130}Sn and 10^4 ions/s for ^{134}Sn** (as requested for IS654 [24]).

isotope	transition	counts/hour	counts/run
^{130}Sn	$2_1^+ \to 0_{\mathrm{g.s.}}^+$	370	$35 \cdot 10^3$
	$4_1^+ \to 2_1^+$	2	200
^{134}Sn	$2_1^+ \to 0_{\mathrm{g.s.}}^+$	15	3530
	$4_1^+ \to 2_1^+$	0,3	73

Table 2: *Calculated γ-ray yields following Coulomb excitation of ^{130,134}Sn. Numbers in rightmost column are given for 12 shifts of ^{130}Sn beam time and 15 shifts ^{134}Sn beam time.*

Slow extraction from the EBIS is requested to reduce the instantaneous particle rate. Taking into account the cross sections from Table 1, the count rate of the particle detectors will be 26 counts/s corresponding to about 26 kHz within the pulse (assumed pulse length 1 ms and an EBIS rate of 5 Hz) which can be processed by the individual DSSSDs.

The CD detector is divided in 2.5° bins (annular strips). Hence, the obtained statistics should allow to split the data set in angular bins adapted to scattered projectiles and recoiling target nuclei.

With the expected beam currents the γ-particle coincidence rates and the expected photopeak intensities are given in Table 2. A ^{206}Pb target of 2 mg/cm^2 for ^{130}Sn and 4 mg/cm^2 for ^{134}Sn (same target as for IS548 [23, 29]) was assumed. The target thickness of 2 mg/cm^2 for ^{130}Sn will allow for a superior separation of scattered reaction partners. Integrated cross sections for excitation of the 2_1^+ and 4_1^+ states are given in Table 1. Energy dependent MINIBALL detection efficiencies are taken from [16] for the individual transitions. The experiment will be separated in two runs with a beam time request of **15 shifts for ^{130}Sn** and **15 shifts for ^{134}Sn**, respectively (Table 2, rightmost column). The 15 shifts for ^{130}Sn will be divided into 12 shifts for beam on target. (Numbers in Table 2 are given for 12 shifts.) Three shifts are requested for a careful diagnosis of the ^{130}Sn beam composition. In this way systematic errors from a potential beam contribution of the isomeric 7^- state in ^{130}Sn will be addressed. The previous experiment did not report on this potential difficulty [6, 7].

The requested shifts will allow to determine the $B(E2; 0_{\mathrm{gs}}^+ \to 2_1^+)$ values in ^{130,134}Sn with a statistical error below 2%. There will be a first time opportunity to determine the $B(E2; 2_1^+ \to 4_1^+)$ value in ^{130}Sn with an error of $\approx 7\%$, and an error of $\approx 12\%$ in ^{134}Sn.

We propose to measure the $B(E2; 0_{\mathrm{gs}}^+ \to 2^+)$ values for the neutron-rich isotopes ^{130,134}Sn. The error of the $B(E2; 0_{\mathrm{gs}}^+ \to 2^+)$ values of the previous experiment is 17 % [7]. We aim to improve this error to below 5 %. The impact of the diagonal matrix elements (not discussed in [7]) will be included. In addition, the $B(E2; 2^+ \to 4^+)$ value will be accessible and will be determined in this region for the first time. Electric quadrupole moments Q_2 can be extracted from the experimental data. For short-lived states, this quantity is only accessible by safe Coulomb excitation via the reorientation effect. Potentially, a candidate for the first 3^- octupole state could be observed adding to a comprehensive understanding of this neutron-rich region.

It is noteworthy that the amount of information on the evolution of collectivity in this region accessible by our experiment can hardly be obtained by other methods and complementary approaches. Lifetime measurements do not allow for determination of diagonal matrix elements. Also, the yields obtainable in fission isomer decay spectroscopy, see [30], are by far not sufficient for a fast-timing analysis. The Sn isotopes are anyway only very weakly populated in neutron-induced or spontaneous fission of actinides. Low-energy beams of neutron-rich Sn isotopes are available with highest intensity exclusively at HIE-ISOLDE. Coulomb excitation at intermediate and relativistic beam energies is a single step process and it is mostly independent of the excitation energy. Investigations of the first 4^+ state are not feasible with this technique.

In summary, Coulomb excitation of ^{130,134}Sn is proposed in order to obtain the electromagnetic matrix elements within high precision. The measurement of the $B(E2, 0_{gs}^+ \to 2^+)$ values in both isotopes will be crucial for understanding the nuclear structure of Sn isotopes around the $N = 82$ shell closure and experimental verification of new predictions from theory.

In total we ask 15 (12+3) shifts for ^{130}Sn and 15 shifts for ^{134}Sn.

References

[1] I. Arcavi et al., Nature 551, 64 (2017); M. R. Drout et al., Science 10.1126/science.aaq0049 (2017); many more.

[2] T. Togashi et al., Phys. Rev. Lett. 121, 062501 (2018).

[3] J. Cederkäll et al., Phys. Rev. Lett. 98, 172501 (2007).

[4] A. Ekström et al., Phys. Rev. Lett. 101, 012502 (2008).

[5] P. Doornenbal et al., Phys. Rev. C 78, 031303(C) (2008).

[6] D.C. Radford, et al Nucl. Phys. A 752 (2005) 264c272c.

[7] R. L. Varner et al., Eur. Phys. J. A 25, s01, 391 (2005).

[8] D. Rosiak et al., Phys. Rev. Lett. 121, 252501 (2018).

[9] J.Terasaki, J.Engel, W.Nazarewicz, M.Stoitsov, Phys. Rev. C 66 (2002) 054313.

[10] S. Sarkar and M. Saha Sarkar, Phys. Rev. C 78, 024308 (2008).

[11] M. P. Kartamyshev et al., Phys. Rev. C 76, 024313 (2007).

[12] A. Covello et al., J. Phys.: Conf. Ser. 267, 012019 (2011).

[13] J. D. Holt et al., J. Phys. G: Nucl. Part. Phys. 39, 085111 (2012).

[14] S. Sarkar and M. Saha Sarkar, J. Phys.: Conf. Ser. 267, 012040 (2011).

[15] J.R. Beene, et al.; Nucl. Phys. A 746 (2004) 471c

[16] N. Warr et al., Eur. Phys. J. A 49, 40 (2013).

[17] V. Bildstein et al., Eur. Phys. J. A 48, 85 (2012).

[18] J. F. Ziegler, `http://www.srim.org`

[19] G. Pasquali et al., Nucl. Instr. Meth. A 405, 39 (1998).

[20] J. M. Allmond et al., Phys. Rev. C 84, 061303(R) (2011).

[21] U. C. Bergmann et al., Nucl. Instr. Meth. B 204, 220 (2003).

[22] J. Terasaki Phy. Rev. C 66, 054313 (2002).

[23] Th. Kröll et al., CERN-INTC-2019-011 / INTC-SR-070.

[24] Th. Kröll et al., CERN-INTC-2019-006 / INTC-SR-065.

[25] `http://www.nndc.bnl.gov`.

[26] U. Koester et al., Nucl. Instr, Meth. B 266, 4229 (2008).

[27] Th. Kröll et al., CERN-INTC-2012-042 / INTC-P-343.

[28] T. Stora, private communication.

[29] C. Henrich, doctoral thesis (TU Darmstadt, 2021).

[30] G. S. Simpson et al., Phys. Rev. Lett. 113, 132502 (2014).

Appendix

DESCRIPTION OF THE PROPOSED EXPERIMENT

The experimental setup comprises:

Part of the	Availability	Design and manufacturing
(fixed ISOLDE installation: MINIBALL + only CD, or MINIBALL + C-REX)	☒ Existing	☒ To be used without any modification
[^{130}Sn experiment/ equipment]	☒ Existing	☐ To be used without any modification ☐ To be modified
	☐ New	☐ Standard equipment supplied by a manufacturer ☐ CERN/collaboration responsible for the design and/or manufacturing
[^{134}Sn experiment/ equipment]	☒ Existing	☐ To be used without any modification ☐ To be modified
	☐ New	☐ Standard equipment supplied by a manufacturer ☐ CERN/collaboration responsible for the design and/or manufacturing

HAZARDS GENERATED BY THE EXPERIMENT (if using fixed installation:) Hazards named in the document relevant for the fixed [MINIBALL + only CD, MINIBALL + T-REX] installation.

Additional hazards:

Hazards	[Part 1 of experiment/ equipment]	[Part 2 of experiment/ equipment]	[Part 3 of experiment/ equipment]
Thermodynamic and fluidic			
Pressure	[pressure][Bar], [volume][l]		
Vacuum			
Temperature	[temperature] [K]		
Heat transfer			
Thermal properties of materials			
Cryogenic fluid	[fluid], [pressure][Bar], [volume][l]		
Electrical and electromagnetic			
Electricity	[voltage] [V], [current][A]		
Static electricity			
Magnetic field	[magnetic field] [T]		
Batteries	☐		
Capacitors	☐		
Ionizing radiation			
Target material [material]			
Beam particle type (e, p, ions, etc)	^{130}Sn	^{134}Sn	
Beam intensity at MINIBALL	10^6 ions/s	10^6 ions/s	
Beam energy	4.4 MeV/u	4.4 MeV/u	
Cooling liquids	[liquid]		
Gases	[gas]		
Calibration sources:	☐		

• Open source	☐		
• Sealed source	☒ [ISO standard]		
• Isotope standard sources	^{60}Co, ^{152}Eu		
• Activity (sources are available)			
Use of activated material:			
• Description	☐		
• Dose rate on contact and in 10 cm distance	[dose][mSV]		
• Isotope			
• Activity			
Non-ionizing radiation			
Laser			
UV light			
Microwaves (300MHz-30 GHz)			
Radiofrequency (1-300 MHz)			
Chemical			
Toxic	[chemical agent], [quantity]		
Harmful	[chem. agent], [quant.]		
CMR (carcinogens, mutagens and substances toxic to reproduction)	[chem. agent], [quant.]		
Corrosive	[chem. agent], [quant.]		
Irritant	[chem. agent], [quant.]		
Flammable	[chem. agent], [quant.]		
Oxidizing	[chem. agent], [quant.]		
Explosiveness	[chem. agent], [quant.]		
Asphyxiant	[chem. agent], [quant.]		
Dangerous for the environment	[chem. agent], [quant.]		
Mechanical			
Physical impact or mechanical energy (moving parts)	[location]		
Mechanical properties (Sharp, rough, slippery)	[location]		
Vibration	[location]		
Vehicles and Means of Transport	[location]		
Noise			
Frequency	[frequency],[Hz]		
Intensity			
Physical			
Confined spaces	[location]		
High workplaces	[location]		
Access to high workplaces	[location]		
Obstructions in passageways	[location]		
Manual handling	[location]		
Poor ergonomics	[location]		

Hazard identification:

none